Eur. Phys. J. A **32**, 149–158 (2007)
DOI 10.1140/epja/i2007-10382-9

THE EUROPEAN PHYSICAL JOURNAL A

Regular Article – Nuclear Structure and Reactions

Decay of 1.643 h ^{95}Ru and its daughter's level structure

Shen Shuifa[1,2,3,a], Fang Keming[4], Gu Jiahui[4], Liu Qingcheng[2], and Xu Furong[1]

[1] School of Physics, Peking University, Beijing 100871, PRC
[2] School of Nuclear Engineering and Technology, East China Institute of Technology, Fuzhou 344000, Jiangxi, PRC
[3] CCAST (World Lab.), P.O. Box 8730, Beijing 100080, PRC
[4] Shanghai Institute of Applied Physics, The Chinese Academy of Sciences, Shanghai 201800, PRC

Received: 10 April 2007
Published online: 21 May 2007 – © Società Italiana di Fisica / Springer-Verlag 2007
Communicated by D. Guerreau

Abstract. The decay of ^{95}Ru has been investigated by means of γ-ray spectroscopy. The ^{95}Ru nuclei were produced by the reaction ^{92}Mo$(\alpha, \mathrm{n})^{95}$Ru at a beam energy of 17 MeV. High-purity Ge detectors have been used singly and in coincidence to study γ-rays in the decay of ^{95}Ru to ^{95}Tc. 132 γ-rays are reported, among them, energies and intensities for 127 transitions have been determined. A decay scheme of ^{95}Ru with 31 levels is proposed which accommodates 127 of these transitions. Spins and parities for three new levels are proposed from calculated log ft values, measured γ-ray branching ratios, and in-beam experiment results of the daughter nucleus ^{95}Tc. Combining with the high-spin states observed by in-beam γ-ray spectroscopy of previous decay works, the structure of the excited states of ^{95}Tc is discussed in the framework of the projected shell model.

PACS. 23.20.Lv γ transitions and level energies – 27.60.+j $90 \leq A \leq 149$ – 21.60.Cs Shell model

1 Introduction

Nuclei with $Z \approx 40$ and $N \approx 50$ have been the subject of much theoretical study. A survey has revealed the fact that no recent experimental information is to be found in the literature concerning the decay scheme of this ^{95}Ru isotope. To be more specific, the last published paper [1], which is widely reported, is more than 30 years old. This serious inadequacy has motivated the need for new, more accurate, measurements in this field. Moreover, the γ-ray spectrum found by Xenoulis *et al.* [2] and Krämer *et al.* [1] was too complex to be satisfactorily resolved by their Ge(Li)-Ge(Li) coincidence data. The availability of larger, more efficient HPGe detectors and the general theoretical interest in nuclei near the $N = 50$ closed shell made HPGe-HPGe coincidence measurements attractive.

In this work the results of our investigation on the ^{95}Tc isotope in radioactive decay are presented. Preliminary results of this work have been published elsewhere [3]. This paper is organized as follows: in sect. 2 the experimental procedures are presented. Section 2.1 reports on the preparation of the ^{95}Ru source. Section 2.2 reports on the results of singles and coincidence measurements. The model-independent level scheme construction, $\beta^+ + \mathrm{EC}$ decay branching ratios and spin-parity assignments are presented in sect. 3. In sect. 4 some concepts of the projected shell model are briefly presented, then the procedure and the result from calculations for both positive- and negative-parity states are presented and compared with known experimental data. Finally, the paper is summarized in sect. 5.

2 Experimental procedures

2.1 Preparation of the sources

The ^{95}Ru samples were prepared by the ^{92}Mo$(\alpha, \mathrm{n})^{95}$Ru reaction utilizing the 17 MeV α from the energy variable cyclotron ($K = 40$) at Shanghai Institute of Applied Physics (SINAP) (formerly called Shanghai Institute of Nuclear Research (SINR)) on 10 mg targets of metal ^{92}Mo isotopically enriched to 99%. The optimal bombarding energy for the yield of ^{95}Ru was estimated on the basis of the excitation function calculated by the computer code ALICE [4]. The only detectable radioactive contaminants in the sources were ^{95}Tc($^{95\mathrm{m}}$Tc $T_{1/2} = 61$ d, $^{95\mathrm{g}}$Tc $T_{1/2} = 20.0$ h) and ^{97}Ru($T_{1/2} = 29$ d), which were formed from the reactions ^{92}Mo$(\alpha, \mathrm{p})^{95}$Tc and ^{94}Mo$(\alpha, \mathrm{n})^{97}$Ru, respectively. In addition, the $^{95\mathrm{m,95g}}$Tc were also formed by the decay of ^{95}Ru. The competing activities had half-

[a] e-mail: shfshen@ecit.edu.cn

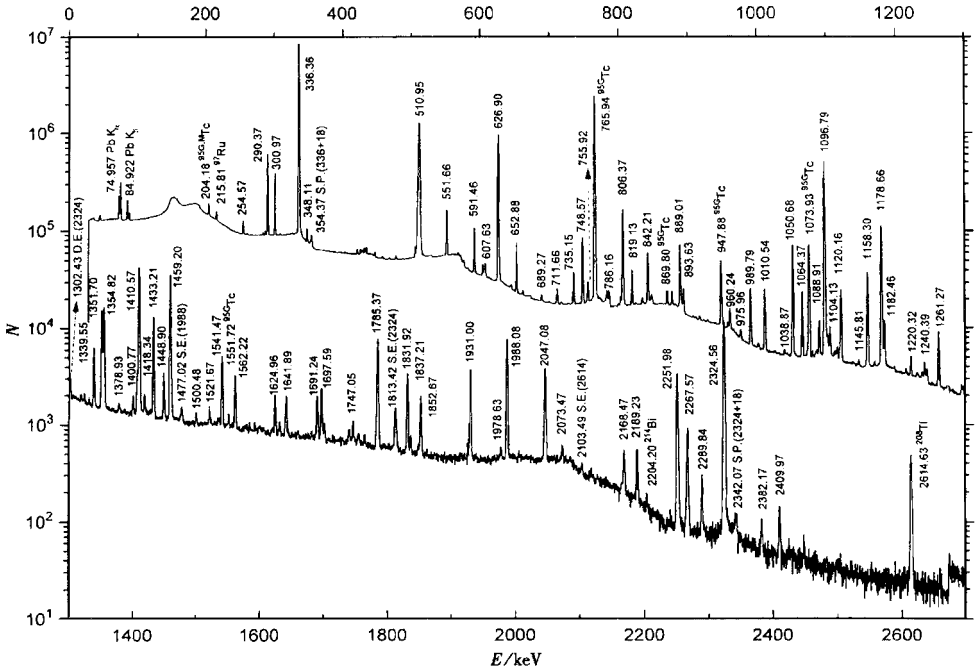

Fig. 1. Gamma-ray singles spectrum recorded with 20% HPGe detector. Peaks labelled with energy only were observed to decay with a half-life of 99 ± 10 min and therefore assigned to ^{95}Ru decay. Prominent background lines are labelled by source as well as energy. S. E., D. E. and S. P. denote the single-escape peak, the double-escape peak and the summing peak, respectively.

lives which differed by more than 18 h from that of ^{95}Ru, so were easily distinguished.

2.2 Experimental methods

2.2.1 Singles spectrum measurement

The singles spectra were measured with a planar HPGe detector (GMX-20190) with 20% efficiency. This HPGe detector had a resolution (full width at half maximum (FWHM)) of 1.90 keV at 1332 keV. The sources were placed at a distance of 10.0 cm from the detector and the counting rate was controlled to be less than 4000 cps. The energy and relative efficiency calibrations were performed with ^{152}Eu and ^{56}Co sources placed at the target position.

2.2.2 Coincidence measurement

The coincidence measurements were carried out using two high-purity Ge detectors with active volumes of 115 cm^3 and 232 cm^3 in order to establish the relation among the γ-rays observed. The detectors were oriented at 90° to minimize annihilation-radiation coincidences. To minimize the crystal-to-crystal scattering an ~ 1.2 cm Pb absorber was placed between the two detectors. One was the same detector as the one used for singles spectrum measurement and placed 8.0 cm from the target, the other was a coaxial HPGe detector (GEM-50195) with 50% efficiency and 1.95 keV resolution at 1332 keV and also placed 8.0 cm from the target. The coincidence data were obtained using a standard fast-slow coincidence circuit, this fast-slow circuit had a time resolution of about 20 ns when gated at ^{60}Co full energy peaks. For low-energy transitions it can be much larger. The coincidence data were recorded event by event on a magnetic tape, each event include one time parameter and two energy parameters of 8192 channels. A total of about 3.7×10^6 coincidence events were accumulated and stored onto magnetic tapes for further analysis.

3 Results

A singles spectrum of the γ-rays from ^{95}Ru is shown in fig. 1. Such spectra have been obtained by counting five ^{95}Ru sources for five hours each started ~ 1 h cooling after the end of bombardment. These summed spectra were analyzed carefully with a computer program which fits each peak with an adjustable line shape (approximately Gaussian) then calculates the peak area and the centroid channel [5], and lines with a half-life 99 ± 10 min were assigned to ^{95}Ru decay. The γ-rays from the ^{95}Ru decay are summarized in table 1. The first and the third columns give the γ-ray energies and relative intensities as established in this work. The energies are given in keV and the relative intensities are normalized with respect to the intensity of the 336.36 keV γ-ray taken as 71.0. The second column gives the initial levels from which the γ-rays depopulate.

The reconstruction of coincidence spectra was performed off-line. For each gate, a gross spectrum with-

Table 1. Energy, initial level, and relative intensity of the γ-rays following ^{95}Ru decay.

Energy (keV)[a)]	Initial level (keV)	Relative intensity[a)]
[g)]35.72[b)] 15		0.021 2
38.9	39.05	
157.05[f)] 15	1085.065	0.030 3
254.57 4	1433.222	0.23 1
260.10[b)] 7	928.004	0.023 2
283.62[b)] 6	1691.332	0.037 2
287.29[b)] 5	1978.61	0.046 2
290.37 4	626.959	3.74 6
300.97 5	928.004	2.22 2
336.36 5	336.507	71.0 6
[g)]338.14[b)] 5		0.68 1
348.11 9	1433.222	0.23 1
403.58[f)] 18	2382.12	0.024 4
421.15 7	2168.425	0.082 4
446.30[d)] 5	2086.18	0.061 4
454.99[b)] 12	1888.238	0.019 2
457.84 8	1085.065	0.039 4
477.14 6	2168.425	0.055 7
505.17 3	1433.222	0.16 1
545.37[b)] 9	1978.61	0.013 3
551.66 3	1178.660	1.59 2
560.12[d)] 7	2251.89	0.018 3
564.09[b)] 7	2203.81	0.042 3
568.34[b)] 5	1747.106	0.081 5
572.12[d)] 4	1785.373	0.082 3
576.22[d)] 4	2267.547	0.060 4
591.46 5	928.004	1.14 3
606.22 6	1691.332	0.11 1
607.63 1	646.68	0.20 1
626.90 5	626.959	15.9 4
628.90 5	667.91	0.36 1
652.88 5	2086.18	0.94 2
662.00[e)] 7	1747.106	0.042 4
689.27 9	2328.84	0.072 4
711.66 8	1639.76	0.155 6
735.15 8	2168.425	0.41 2
748.59 8	1085.065	1.44 4
755.92 8	2189.199	0.25 1
781.68[b,h)]	2189.199	
786.16[d)] 10	1433.222	0.072 5
803.16[b)] 10	1888.238	0.089 3
806.37 9	1433.222	3.37 6
819.13 7	1747.106	0.55 1
834.52[d)] 11	2267.547	0.074 5
842.21 9	1178.660	1.01 2
844.96[b,h)]	2251.89	
876.75 7	1213.23	0.17 1

Table 1. Continued.

Energy (keV)[a)]	Initial level (keV)	Relative intensity[a)]
889.01 7	928.004	1.46 4
891.27 8	2324.596	0.060 4
893.63 7	1978.61	0.29 1
917.13[b)] 11	2324.596	0.029 4
957.17[c)] 4	957.18	0.045 2
960.24 4	1888.238	0.18 1
975.96[e)] 6	2189.199	0.057 3
989.79 4	2168.425	0.57 1
1001.41[b)] 10	2086.18	0.028 3
1010.54 4	2189.199	0.59 1
1038.87[b)] 9	2251.89	0.019 3
1050.68 5	1978.61	2.07 2
1064.37 5	1691.332	0.58 1
1070.81[b,h)]	1407.61	
1079.15[b)] 9	1747.106	0.025 2
1084.96 13	1085.065	0.018 2
1088.91 7	2267.547	0.22 1
1096.79 5	1433.222	16.4 2
1100.49[d)] 7	1747.106	0.028 2
1104.13 5	2189.199	0.14 1
1111.37[b)] 9	2324.596	0.026 2
1118.69[b)] 8	2203.81	0.052 2
1120.17 5	1747.106	0.69 2
1145.81[b)] 9	2324.596	0.022 3
1158.30 5	1785.373	0.53 3
	2086.18	0.70 3
1168.58[b)] 12	2382.12	0.015 3
1178.66 2	1178.660	3.94 5
1182.47 2	2267.547	0.30 1
1213.17 10	1213.23	0.017 2
1220.32 6	1888.238	0.069 4
1237.08 7	1276.13	0.020 1
1240.39 2	2168.425	0.063 2
1243.73 3	2328.84	0.042 2
1261.27 1	1888.238	0.26 1
1294.69[b)] 5	2251.89	0.022 1
1297.02[b)] 5	2382.12	0.019 1
[g)]1319.31[b)] 13		0.011 1
1324.00[e)] 10	2251.89	0.015 2
1331.75[b,f)] 12	1978.61	0.011 2
1339.55 4	2267.547	0.20 1
1351.70 4	1978.61	0.61 1
1354.82 4	1691.332	0.66 1
[g)]1378.93[b)] 13		0.017 2
1400.77 7	2328.84	0.031 2
1407.55[b)] 6	1407.61	0.091 2
1410.57 5	1747.106	1.90 2
1418.34 8	2086.18	0.033 2
1433.21 5	1433.222	0.56 1
1448.90 6	1785.373	0.11 1
1459.20 4	2086.18	1.66 6
1500.48[b)] 10	2168.425	0.013 2
1521.66[c)] 8	2168.425	0.027 2
1541.47 4	2168.425	0.21 1
1562.22 4	2189.199	0.11 1
1620.40[b,f,h)]	2267.547	

Table 1. Continued.

Energy (keV)[a)]	Initial level (keV)	Relative intensity[a)]
1624.96 5	2251.89	0.063 3
1632.13 9	1632.13	0.015 1
1641.89 5	1978.61	0.079 4
1661.04[b)] 18	2328.84	0.005 2
1691.24 5	1691.332	0.074 3
1697.59 5	2324.596	0.096 4
1701.75[f)] 8	2328.84	0.020 1
1747.05 8	1747.106	0.025 2
1755.57 13	2382.12	0.011 2
1783.12[b)] 7	2410.05	0.020 1
1785.37 2	1785.373	0.45 1
1831.92 2	2168.425	0.19 1
1837.21 7	1837.21	0.017 1
1848.98[b,f)] 13	1888.238	0.008 1
1852.67 3	2189.199	0.095 3
1931.00 2	2267.547	0.24 1
1978.63[f)] 12	1978.61	0.0086 7
1988.08 2	2324.596	0.50 1
2047.08 5	2086.18	0.26 1
2073.47[b)] 12	2410.05	0.013 2
2168.47 8	2168.425	0.028 2
2189.23 7	2189.199	0.032 2
2251.98 5	2251.89	0.27 1
2267.57 6	2267.547	0.073 3
2289.84 6	2328.84	0.018 1
2324.56 5	2324.596	1.01 3
2382.17 13	2382.12	0.007 1
2409.97 10	2410.05	0.010 1
[g)]2424.45[b)] 31		0.0015 3

a) The reported errors refer to the last significant digits.
b) New γ-transition identified in the present work.
c) ^{95}Tc transition not assigned to the level scheme before, but placed into the decay scheme now.
d) The placement of the γ-transition confirmed again in the present work.
e) The placement of the γ-transition changed in the present work.
f) The placement of the γ-transition is uncertain.
g) Not placed in the decay scheme.
h) γ-transition detected in coincidence spectra only, so its relative intensity is not given.

out random coincidence and background correction and a background spectrum were both obtained. A coincidence relationship was determined by comparing this pair of spectra. A total of 84 coincidence spectra have been evaluated. Some selected spectra are presented in fig. 2a-f. Almost all transitions determined in singles spectra have appeared in coincidence spectra. On the other hand, several weak peaks that cannot be separated in singles spectra were also identified in coincidence spectra. These are 781.68, 844.96, 1070.81, and 1620.40 keV γ-rays (cf. fig. 2a-b), and they are also listed in table 1, their relative intensities are not given.

Experimental data analysis demonstrated that there are one hundred and thirty-two γ-rays assigned to ^{95}Tc. Seven γ-rays at 446.30, 560.12, 572.12, 576.22, 786.16, 834.52, and 1100.49 keV are confirmed again. Thirty-four new γ-rays have been identified, and they are shown in table 1 labelled b). The 662.2 and 976.2 keV γ-rays have been assigned tentatively by Xenoulis *et al.* [2] to de-excite the level at 2409.3 keV excitation. In the present work, however, the 662.00 keV γ-ray has been observed in coincidence with the 748.59 keV γ-ray (cf. fig. 2d), and the 975.96 keV γ-ray has been observed in coincidence with the 876.75 keV γ-ray (cf. fig. 2e), so they have been assigned to de-excite two levels at 1747.106 and 2189.199 keV excitation, respectively. Three new levels at 957.18, 1407.61, and 2203.81 keV are assigned. There are five relatively weak γ-rays which were observed to decay with a half-life of ^{95}Ru and can reasonably be assigned to ^{95}Ru decay although a place in the decay scheme could not be found for them at the present time, and they are also shown in table 1 labelled g). The proposed scheme for the decay of 1.643 h ^{95}Ru, from the evidence presented above, is shown in fig. 3 and the arguments for its construction are summarized below.

A new level has been assigned at 957.18 keV. One γ-ray at 957.17 keV has been assigned to de-excite this level. Thus, the 957.17 keV γ-ray has been observed in coincidence with the 1294.69 keV γ-ray, and it has been assigned to depopulate the level at 2251.89 keV excitation. A second new level has been assigned at 1407.61 keV excitation. One γ-ray transition at 1407.55 keV has been assigned to de-excite this level. Specifically, this γ-ray has been observed in coincidence with the 283.62, 781.68, 844.96, and 917.13 keV γ-rays, respectively (cf. fig. 2a-b), and they have been assigned to depopulate the four levels at 1691.332, 2189.199, 2251.89, and 2324.596 keV excitation, respectively. A third new level has been assigned at 2203.81 keV excitation. Two γ-rays at 564.09 keV and 1118.69 keV have been assigned to de-excite this level. These two γ-rays have been seen in coincidence with the 711.66 keV and 748.59 keV γ-rays, respectively, and they have been assigned to depopulate the two levels at 1639.76 keV and 1085.065 keV excitation, respectively (cf. fig. 2c-d).

As to the $J\pi$ values assignments of these levels, the first forbidden decays in this mass range have $\log ft \geq 8$ [6], so the β-decay branches with $\log ft \leq 7$ are assumed to be allowed transitions which populate positive-parity levels with $J = 3/2$, $5/2$, or $7/2$, since $J\pi = 5/2^+$ for ^{95}Ru [7]. Because only $M1$, $E1$ and $E2$ γ-rays should have observable intensity, a direct transition to the $9/2^+$ ground state eliminates the $3/2^+$ possibility. The 2203.81 keV level decays to $(5/2)^+$ and $(3/2^-)$ states, and its $\log ft$ value is 6.05, so $J\pi = 3/2^+$ or $5/2^+$ assignments are possible. The 1407.61 keV level decays to $9/2^+$ and $7/2^+$ states, and states with spin and parity $5/2^+$, $7/2^+$ and $(7/2)^+$ γ-rays feeding this level, so $J\pi = 5/2^-$ or $7/2^-$ assignments are possible. In addition, the spin and parity of the 957.18 keV level is assigned as $11/2^+$ in the in-beam study [8]. In the present work this $J\pi$ value is adopted.

In addition, a level at 1275.86 keV was observed in the $(\mathrm{p}, \mathrm{n}\gamma)$ reaction [9] to de-excite by a 1236.91 keV transition to the 38.9 keV $1/2^-$ isomeric state and by a 608.20 keV

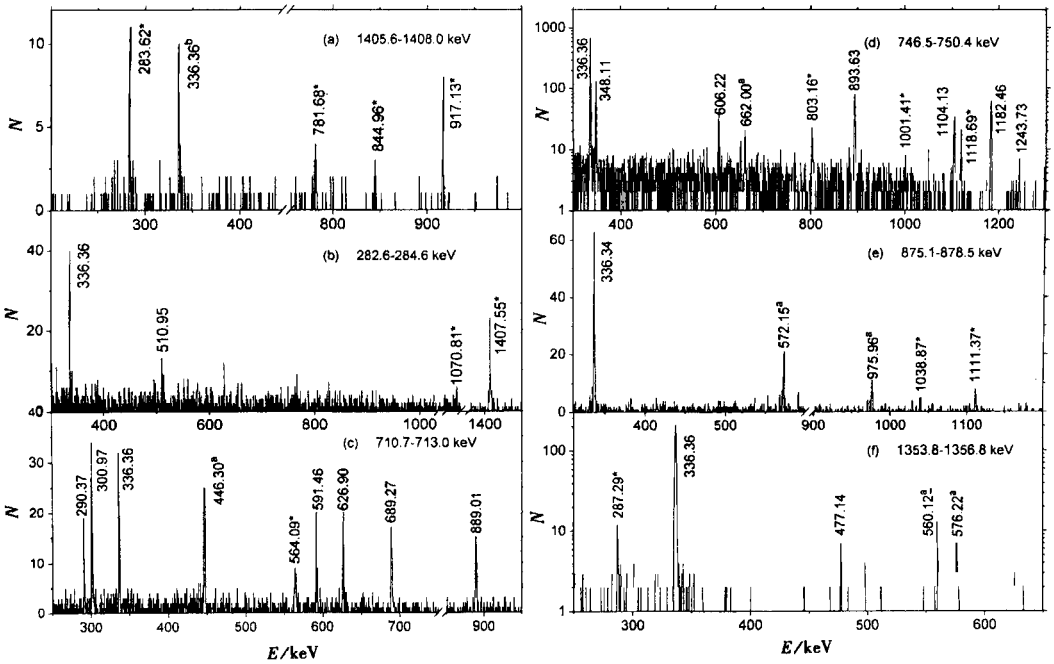

Fig. 2. Some examples of coincidence spectra. The asterisk denotes the new γ-ray, the peak with a means that the placement of the transition is certain, the peak with b is due to random coincidence. (a) Gated at 1405.6–1408.0 keV, (b) gated at 282.6–284.6 keV, (c) gated at 710.7–713.0 keV, (d) gated at 746.5–750.4 keV, (e) gated at 875.1–878.5 keV, (f) gated at 1353.8–1356.8 keV.

transition to the 667.79 keV $5/2^-$ state. In this work the 1237.08 keV γ-ray observed in the ^{95}Ru decay was tentatively assigned to de-excite this 1276.13 keV level, although no coincidence information supporting or contradicting this assignment was found. The $J\pi$ assignment for this 1276.13 keV level is $3/2^-$ [9]. A level at 1631.97 keV excitation has been assigned in ref. [9] and the 1631.97 keV and 750 keV γ-rays have been assigned to de-excite this level to the ground state and the 882.10 $13/2^+$ state, respectively. In the present work the 1632.13 keV γ-ray observed in the ^{95}Ru decay was tentatively assigned to de-excite this 1632.13 keV level. The probable $J\pi$ values for this 1632.13 keV level are $9/2^+$ or $11/2^+$. Sarantites and Xenoulis [9] tentatively assigned a level at 1837.5 keV which decays via a transition of 1837.7 keV to the ground state and a transition of 1501.3 keV to the 336.40 keV $7/2^+$ state, and this is confirmed by Minehara and Mitarai [10], so the level at 1837.21 keV excitation to de-excite by the 1837.21 keV transition has been adopted in this work. The $J\pi$ value of 1837.5 keV is assigned as $7/2^+$ or $9/2^+$ in the $(\mathrm{p}, \mathrm{n}\gamma)$ reaction [10]. In the present work this $J\pi$ value is adopted.

Relative $(\beta^+ + \mathrm{EC})$ decay strength (relative to 71.0 for the 336.36 keV γ-ray) to each energy level can be obtained from the transition deficits (transition intensity from a level minus the intensity to that level). The renormalization coefficient (1.032 ± 8) was then obtained by requiring that the sum of the intensities of the $(\beta^+ + \mathrm{EC})$ branches feeding to the ^{95}Tc should be equal to 1 (100%). The absolute intensities of γ-rays and the percent population of the levels in ^{95}Tc by β^+ decay and electron capture are given in fig. 3. In the present work the half-life value $T_{1/2} = 1.643 \pm 0.014$ h is adopted [11]. Finally, basing on the 2567.1±12.7 keV Q_{EC} value for $(\beta^+ + \mathrm{EC})$ decay, which uses mass values from the 2003 Atomic Mass Evaluation by Audi *et al.* [12], the $\log ft$ values were deduced.

4 The projected shell model description

It is well established by now, both from experimental data and from spherical shell model calculations, that in the $Z \sim 42$–44 region single-particle excitations dominate the level structures of nuclei with $N \leq 51$ even at rather high angular momenta. On the other hand, nuclei with $N \geq 55$ exhibit collective behavior. An example of this region is ^{101}Tc; it has been investigated by our group, and its band structures are reproduced well by the PSM calculations [13]. Until recently, very little was known about the $N = 52$–54 intermediate nuclei. In order to understand these "transitional nuclei", we select the nucleus ^{95}Tc as an example. In this section, we report on our investigation of the level structure in the ^{95}Tc nucleus.

We first review briefly the main properties of the projected shell model and subsequently we compare the calculations with the experimental results. Our study is based on the projected shell model (PSM) [14]. In contrast to the spherical shell models, the projected shell model (PSM) builds its model basis by using deformed (Nilsson type) quasiparticle states. One advantage of this approach is that the dominant nuclear correlations can be incorporated efficiently in the wave functions. Therefore, the PSM can treat the well-deformed nuclei without running into problems related to dimension explosion. The deformed

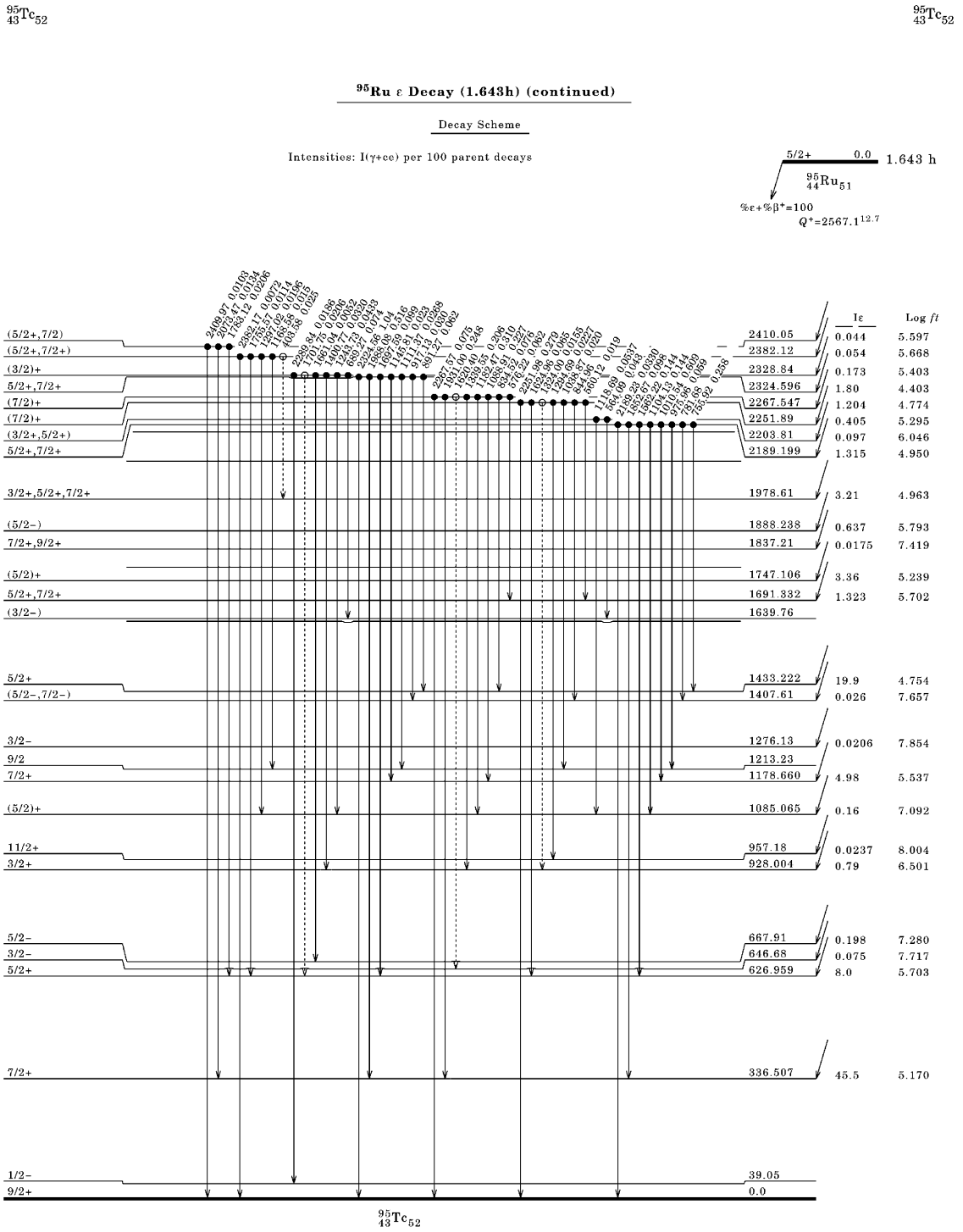

Fig. 3. The decay scheme of ^{95}Ru as established from the present study. The transition energies are labeled in keV. The solid circle denotes placement confirmed by coincidence, and the open circle denotes questionable coincidence. The dotted arrow means that the placement of the transition is not very certain.

Nilsson states violate the angular momentum. However, there are well-established projection techniques which allow a recovery of this quantum number. Thus, a PSM wave function is a linear combination of the angular-momentum projected states given by

$$|\psi_M^I\rangle = \sum_\kappa f_\kappa \hat{P}^I_{MK_\kappa} |\varphi_\kappa\rangle \,. \tag{1}$$

The intrinsic states $|\varphi_\kappa\rangle$ are multi-quasiparticle (qp) states, which include 1- and 3-qp configurations, *i.e.*, they are spanned by the set

$$\left\{a^+_{\rm p}|0\rangle, a^+_{\rm n_1} a^+_{\rm n_2} a^+_{\rm p}|0\rangle\right\}, \tag{2}$$

for odd-proton nuclei. The index κ labels the basis states. These multi-qp states carry the good K quantum num-

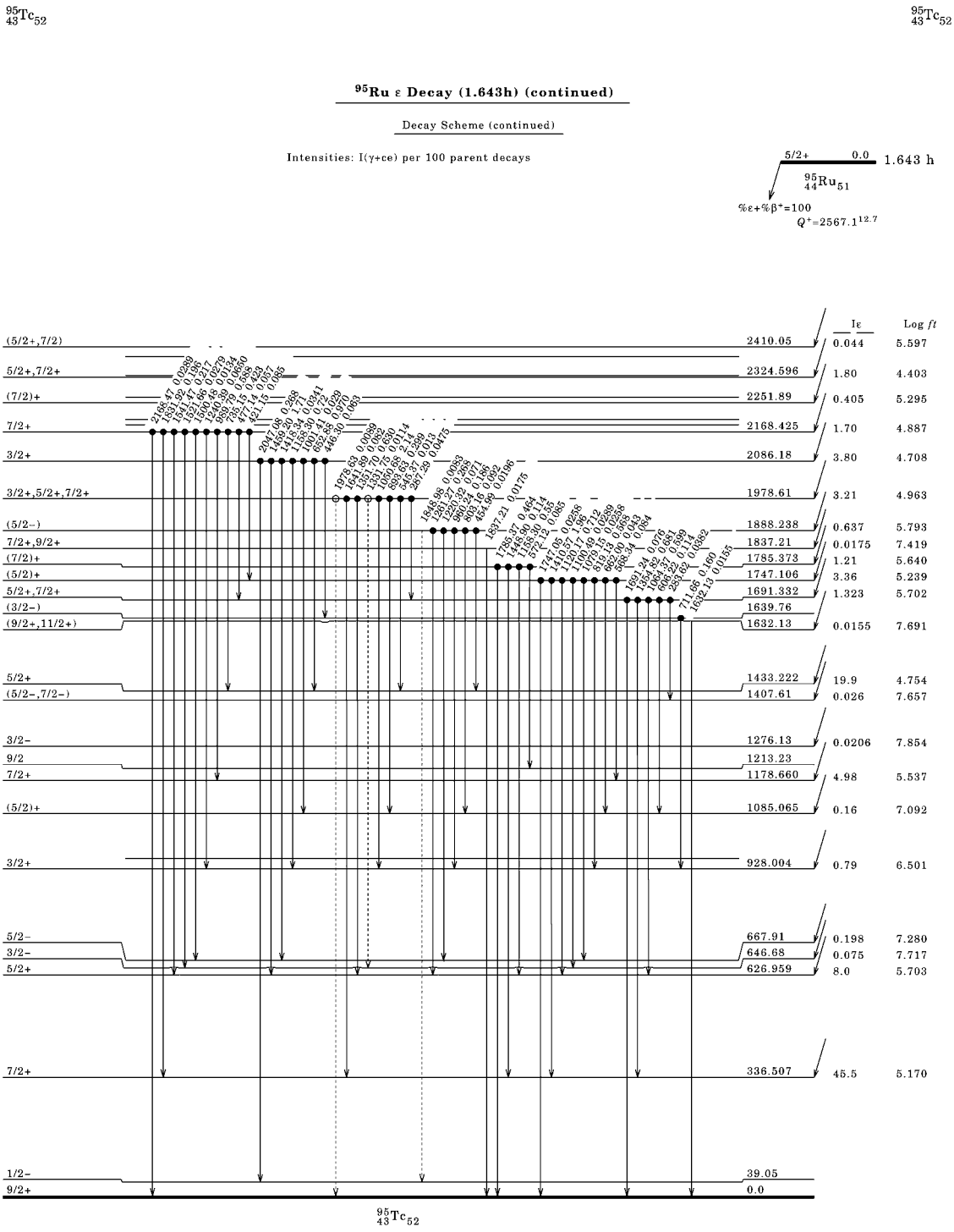

Fig. 3. Continued.

ber originated from the deformed Nilsson single-particle states. The present calculations have been performed by taking into account three full major shells $N = 3$, 4, 5 ($N = 2$, 3, 4) for neutrons (protons), respectively. The PSM employs the pairing plus quadrupole Hamiltonian, with the inclusion of a quadrupole-pairing term [14]. There are several indications that ^{95}Tc is moderately deformed. So our calculations are performed for ^{95}Tc with the basis deformation $\varepsilon_2 = 0.20$. It is interesting to mention that the fact that the PSM prefers the choice of such a deformed basis was discussed in the particle-rotor model point of view [15], and from the comparison of fig. 1 in ref. [15] and fig. 10b in ref. [16] we have found that the deformation parameter δ used by Zeghib is equal to the parameter ε used by Browne *et al.* [16]. The hexadecapole deformation parameter $\varepsilon_4 = -0.007$ is taken from the

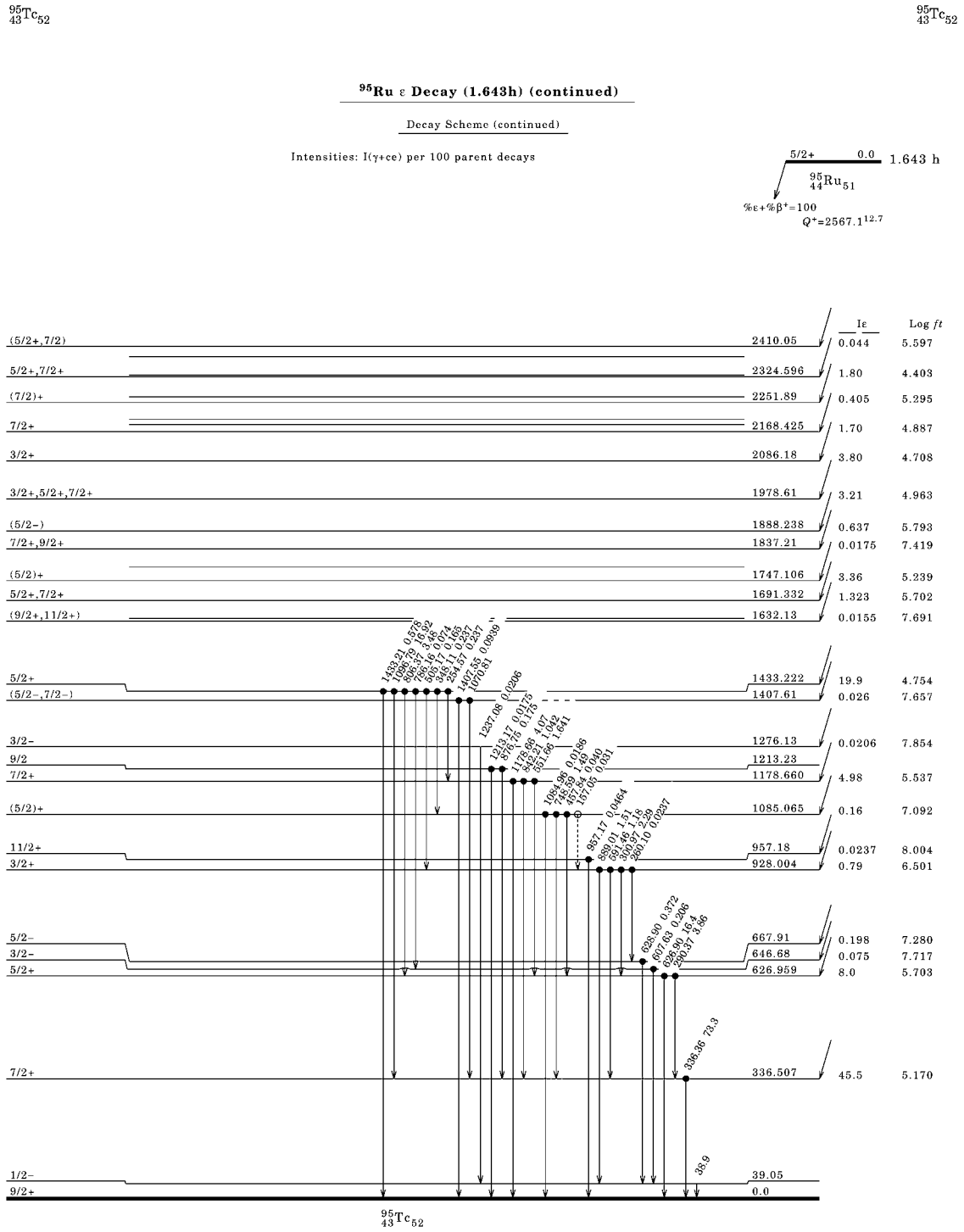

Fig. 3. Continued.

compilation of Möller *et al.* [17]. The experimental data are taken from the present work except that the $13/2^+$ level has been taken from ref. [18].

In the present work, the pairing gaps $\Delta_{\rm p}$ and $\Delta_{\rm n}$ are calculated using the four-point formula as follows [19]:

$$\Delta_{\rm p} = \frac{1}{4}\big\{B(N,Z-2) - 3B(N,Z-1) + 3B(N,Z) - B(N,Z+1)\big\}, \quad (3)$$

$$\Delta_{\rm n} = \frac{1}{4}\big\{B(N-2,Z) - 3B(N-1,Z) + 3B(N,Z) - B(N+1,Z)\big\}. \quad (4)$$

The values of the total nuclear binding energy, B, are taken from ref. [17], and experimental data are adopted if only they can be supplied. It should be pointed out that if the values of the total nuclear binding energy, B, are substituted by the corresponding atomic mass,

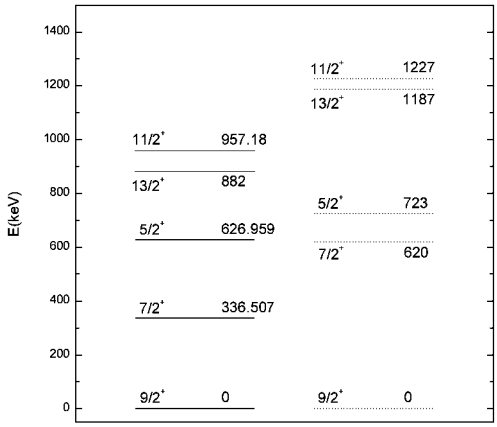

Fig. 4. The comparison of the observed positive-parity states in ^{95}Tc with projected shell model calculations.

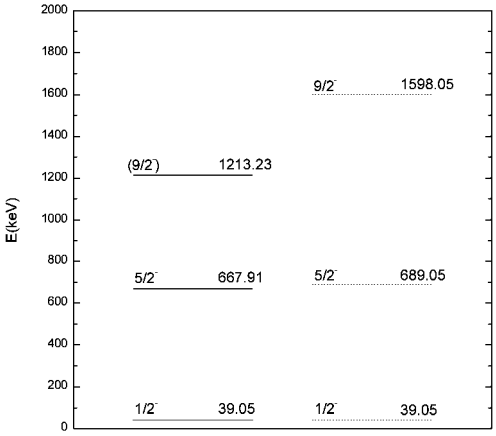

Fig. 5. The comparison of the experimentally observed negative-parity band (solid lines) in ^{95}Tc with the predictions of the PSM (dotted lines).

these two formulae still hold. The results we obtain are $\Delta_{\rm p} = 1.5075\,{\rm MeV}$ and $\Delta_{\rm n} = 0.8425\,{\rm MeV}$. The spin-orbit force parameters, κ and μ, appearing in the Nilsson potential are taken from the compilation of Zhang *et al.* [20], except for those of proton in major shells $N = 3$ and 4, which are taken from ref. [15]. The basis states for the calculation were restricted to the Nilsson states near the Fermi surface. For positive parities all states of $g_{9/2}$ parentage ($1/2^+[440]$, $3/2^+[431]$, $5/2^+[422]$, $7/2^+[413]$, and $9/2^+[404]$) were included, as well as the $1/2^+[431]$ and $3/2^+[422]$ states of $g_{7/2}$ parentage and the $1/2^+[420]$ state of $d_{5/2}$. Figure 4 shows the comparison between the experimental excitation energies and the projected shell model calculations for the positive-parity band. As can be seen, for the positive-parity band of ^{95}Tc, the patterns and order of all calculated levels agree with that of the experimental ones, especially the ordering of the 5/2, 7/2, 9/2 positive-parity states, the so-called anomalous coupling states. Therefore, a satisfactory description for these observations is possible in the present version of the PSM. In the negative-parity band calculations, the configuration space is constructed by selecting the qp states close to the Fermi energy in the $N = 4$ ($N = 3$) major shell for neutrons (protons), *i.e.*, those six Nilsson states with $p_{1/2}$, $p_{3/2}$ and $f_{5/2}$ parentage for protons, the $1/2^-[301]$, $1/2^-[310]$, $1/2^-[321]$, $3/2^-[301]$, $3/2^-[312]$, and $5/2^-[303]$ states, and forming multi-qp states from them. In the present work the negative-parity band, calculated for a slightly larger quadrupole deformation parameter $\varepsilon_2 = 0.225$, seems to yield better agreement with the experiment. The theoretically determined energy of the negative-parity band is compared with the experimental data in fig. 5. The experimental results are fairly close to the theoretical results for the lower-spin states, *i.e.* for $I \leq 9/2^-$. We would like to emphasize here that all these states have been obtained by a single diagonalization, without any adjustment for individual states.

The results show that this simple model with very few parameters can explain successfully most of the structure of ^{95}Tc. We have attempted to show that the basic features of ^{95}Tc can be explained naturally if it is deformed. We would like to emphasize that the deformation of $\varepsilon_2 = 0.20$ suggested in the present work for ^{95}Tc is based primarily on the model analysis of electromagnetic transition properties [15] and it fits into the systematics of other Tc nuclei in previous work [21–23]. Its deformation is intermediate to the strongly deformed and slightly deformed regions, and its structure exhibits features found in both regions.

5 Summary

In summary, an extensive set of low-spin states in ^{95}Tc has been identified from the present ^{95}Ru $\beta^+ + {\rm EC}$ decay work. 1.643 h ^{95}Ru was produced and studied by γ-ray spectroscopy of the $^{92}{\rm Mo}(\alpha, {\rm n})^{95}$Ru reaction; 34 of the 132 observed γ-rays following ^{95}Ru decay are new. According to the coincidence relations, 29 new γ-rays were fitted into the level scheme, the placement of 7 γ-rays in the level scheme was confirmed, 3 new levels were assigned, a modified and expanded decay scheme was proposed. In addition, the structure of excited positive/negative-parity states of ^{95}Tc has been discussed in the framework of the projected shell model. The overall energy agreement between experimental and calculated values is seen to be good. It is interesting to note that our calculation reproduces the experimental data well for the three low-lying levels with $J^\pi = 9/2^+$, $7/2^+$, and $5/2^+$. The interpretation of the structure of ^{95}Tc in the framework of PSM has proven to be successful.

The authors would like to thank the personnel of the cyclotron in Shanghai Institute of Applied Physics for their continued cooperation and assistance in carrying out the bombardment. This project is supported by the Major State Basic Research Development Program in China under Contract No. 2006CB708409, the National Natural Science Foundation of China under Grant Nos. 10547140, 10525520,

10405031, 60476043 and 10475002, the Natural Science Foundation of Jiangxi Province under Grant No. 0612003, and the China Postdoctoral Science Foundation under Grant No. 20060390370.

References

1. K. Krämer, B.W. Huber, Z. Phys. **267**, 117 (1974).
2. A.C. Xenoulis, D.G. Sarantites, Phys. Rev. C **7**, 1193 (1973).
3. Fang Keming, Liu Jingyi, Shi Shuanghui, Gu Jiahui, Zeng Jiping, Yu Xiaohan, Shen Shuifa, Li Yan, High Energy Phys. Nucl. Phys. (in Chinese) **23**, 820 (1999).
4. M. Blann, University of Rochester report, UR NSRL-181 (1978).
5. K. Okano, K. Aoki, Annu. Rep. Res. Reactor Inst. Kyoto Univ. **23**, 24 (1990).
6. C.M. Lederer, J.M. Hollander, I. Perlman, *Table of Isotopes* (Wiley International Publication, New York, 1967).
7. J.B. Ball, Bull. Am. Phys. Soc. **15**, 551 (1970).
8. K.A. Marshall, J.V. Thompson, W.B. Cook, M.W. Johns, Can. J. Phys. **56**, 117 (1978).
9. D.G. Sarantites, A.C. Xenoulis, Phys. Rev. C **10**, 2348 (1974).
10. E. Minehara, S. Mitarai, J. Phys. Soc. Jpn. **48**, 4 (1980).
11. T.W. Burrows, Nuclear Data Sheets **68**, 717 (1993).
12. G. Audi, A.H. Wapstra, C. Thibault, Nucl. Phys. A **729**, 337 (2003).
13. Shen Shuifa, Wang Fengge, Gu Jiahui, Liu Yujuan, Tang Bin, Jiang Weizhou, J. Phys. Soc. Jpn. **75**, 014201 (2006).
14. K. Hara, Y. Sun, Int. J. Mod. Phys. E **4**, 637 (1995).
15. S. Zeghib, Phys. Scr. **67**, 106 (2003).
16. Edgardo Browne, Janis M. Dairiki, Raymond E. Doebler *et al.*, *Table of Isotopes*, edited by C. Michael Lederer, Virginia S. Shirley, seventh edition (Wiley-Interscience Publication, John Wiley & Sons, Inc., New York, Chichester, Brisbane, Toronto) Appendices-38.
17. P. Möller, J.R. Nix, W.D. Myers, W.J. Swiatecki, At. Data Nucl. Data Tables **59**, 185 (1995).
18. K.A. Marshall, J.V. Thompson, W.B. Cook, M.W. Johns, Can. J. Phys. **56**, 117 (1978).
19. Aage Bohr, Ben R. Mottelson, *Nuclear Structure*, Vol. **1** (Benjamin, New York, Amsterdam, 1969) p. 169.
20. J.-Y. Zhang, N. Xu, D.B. Fossan, Y. Liang, R. Ma, E.S. Paul, Phys. Rev. C **39**, 714 (1989).
21. Aslan H. *et al.*, Phys. Rev. C **54**, 576 (1996).
22. Crowe B. *et al.*, Phys. Rev. C **57**, 590 (1998).
23. Savage D.G. *et al.*, Phys. Rev. C **55**, 120 (1997).